

Surface-Induced Dissociation of Noncovalent Protein Complexes in an Extended Mass Range Orbitrap Mass Spectrometer

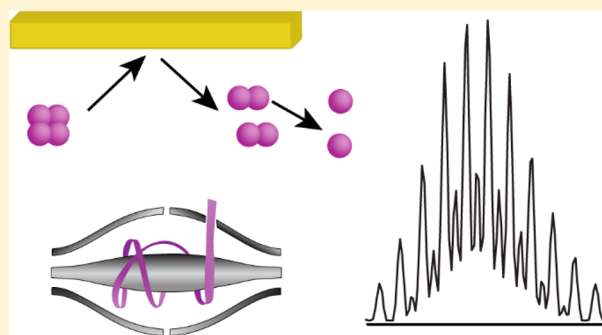
Zachary L. VanAernum,^{†,‡,§} Joshua D. Gilbert,^{†,||,§} Mikhail E. Belov,[‡] Alexander A. Makarov,[‡] Stevan R. Horning,[‡] and Vicki H. Wysocki^{†,*}

[†]Department of Chemistry and Biochemistry and [#]Resource for Native Mass Spectrometry Guided Structural Biology, The Ohio State University, Columbus, Ohio 43210, United States

[‡]Thermo Fisher Scientific, 28199 Bremen, Germany

S Supporting Information

ABSTRACT: Native mass spectrometry continues to develop as a significant complement to traditional structural biology techniques. Within native mass spectrometry (MS), surface-induced dissociation (SID) has been shown to be a powerful activation method for the study of noncovalent complexes of biological significance. High-resolution mass spectrometers have become increasingly adapted to the analysis of high-mass ions and have demonstrated their importance in understanding how small mass changes can affect the overall structure of large biomolecular complexes. Herein we demonstrate the first adaptation of surface-induced dissociation in a modified high-mass-range, high-resolution Orbitrap mass spectrometer. The SID device was designed to be installed in the Q_{Exactive} series of Orbitrap mass spectrometers with minimal disruption of standard functions. The performance of the SID-Orbitrap instrument has been demonstrated with several protein complex and ligand-bound protein complex systems ranging from 53 to 336 kDa. We also address the effect of ion source temperature on native protein–ligand complex ions as assessed by SID. Results are consistent with previous findings on quadrupole time-of-flight instruments and suggest that SID coupled to high-resolution MS is well-suited to provide information on the interface interactions within protein complexes and ligand-bound protein complexes.



Elucidating information about the quaternary structure of biological macromolecular complexes is central to our understanding of biological functions.¹ While X-ray crystallography, NMR, and cryo-electron microscopy are considered the dominant analytical techniques in structural biology, native mass spectrometry has proven itself as an important complementary technique.^{2–4} Although the three former techniques can often obtain atomic resolution structures, native MS carries advantages in sensitivity, speed, tolerance of sample and/or structural heterogeneity, and tolerance of a wide range of molecular sizes. In the field of native MS, time-of-flight (TOF) MS emerged early on as the method of choice for mass analysis.^{5,6} This is due in part to the inherently broad mass range of the TOF mass analyzer, which makes it an obvious choice for the study of large biomacromolecules. Although the TOF analyzer served native MS extremely well for over a decade, higher-resolution instruments equipped with Fourier transform ion cyclotron resonance (FT-ICR) or Orbitrap mass analyzers have become increasingly amenable to the analysis of large biomolecules.^{7–9} Advancements in native MS with Orbitrap platforms have demonstrated the potential of studying systems ranging to the megadalton scale at high resolution.^{10,11}

While important information about a multi-subunit complex such as molecular weight, binding kinetics, etc. can be determined from an MS experiment, the native MS toolbox is further extended through tandem MS (MS/MS) experiments. The power of native MS/MS stems from the ability to introduce noncovalently linked macromolecular complexes into the gas phase, select a specific ion (oligomeric state, ligand-bound state, etc.), and subsequently dissociate that species into subcomplexes prior to mass analysis. This workflow allows the determination of subunit identity, composition, stoichiometry, connectivity, and topology as well as ligand identity, stoichiometry, and binding location within a biomacromolecular complex.^{12–14} A wide range of activation techniques are utilized to probe the structure of protein complexes, each with its own advantages. Collision-induced dissociation (CID) is the most common activation method, as it comes standard on almost all commercially available tandem mass spectrometers. CID involves accelerating ions through a collision cell filled with inert gas such as nitrogen, with enough energy to induce fragmentation of the

Received: December 4, 2018

Accepted: January 28, 2019

Published: January 28, 2019

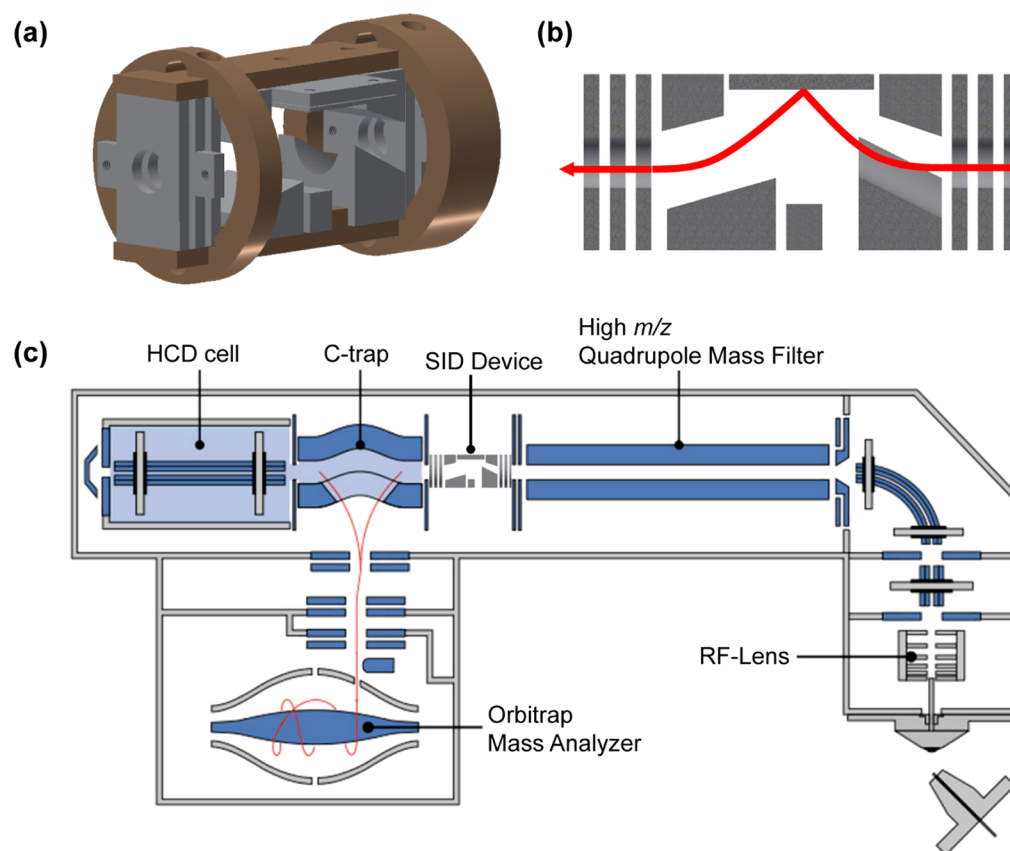


Figure 1. (a) Technical drawing of the SID device with mounting brackets. (b) A simplified cross section depiction of the SID device showing a right-to-left ion trajectory in SID mode. (c) A diagram of the modified EMR platform with the prototype SID device installed between the quadrupole and C-trap.

ion.¹⁵ Subjecting protein complexes to this multistep, incremental energy deposition generally results in the unfolding/restructuring of the complex and ejection of a highly charged monomer, leaving behind the complementary $(n - 1)$ mer with a disproportionately low charge with respect to mass.^{16–18} Such experiments can be leveraged to gain information on stoichiometry and gas phase stability of a given complex.^{15,19} Electron transfer and electron capture dissociation (ETD, ECD) techniques have also been used, often resulting in backbone cleavages within a protein complex, which can be useful for surface mapping and proteoform sequencing,^{7,20–22} and less commonly leading to direct dissociation of the noncovalent complex.²³ Ultraviolet photodissociation (UVPD) has similarly been shown to provide sequence information on protein subunits within a complex and has also been demonstrated to break noncovalent interactions between subunits to yield subcomplexes.^{24–26}

Surface-induced dissociation (SID) has emerged as a powerful collision-based activation method for probing protein complex structures in the gas phase, yielding fragmentation that provides information complementary to that gained from the activation methods mentioned previously.²⁷ Rather than subjecting ions to multiple low-energy collisions with background gas, SID experiments direct ions into an inert, rigid surface to impart energy into the analyte in a single, high-energy step. SID generally results in a more symmetric partitioning of charge in the produced subcomplexes relative to CID²⁸ and UVPD.²⁶ As observed using ion mobility (IM)-MS instruments, subcomplexes generated via SID are generally

compact after dissociation, with collision cross sections reflective of the biomolecular (sub)structures.²⁹ Additionally, SID of ligand-bound protein complexes often results in subcomplexes with ligands retained in the binding pocket, which is often not the case for CID.^{30,31} These features make SID a useful tool to probe biomolecular complexes without solved structures.^{32–34}

Until recently, work involving SID of protein complexes has largely been carried out on TOF platforms.^{35,36} With growing utilization of native MS for structural characterization of protein complexes, it has become apparent that greater mass resolution is often desirable, which would allow for a deeper insight into a given biological system. For example, measurement of mass shifts resulting from post-translational modifications and/or the binding of small ligands or cofactors becomes possible at the protein complex level at sufficient resolution.^{37,38} Each type of mass analyzer (TOF, FT-ICR, Orbitrap) has advantages and disadvantages, and the choice of instrument will often depend on the question being addressed. Our group has recently demonstrated SID on an FT-ICR platform, achieving unparalleled mass resolution of SID-generated subcomplexes.³⁹ However, we believe that activation methods such as SID should be vendor- and platform-neutral and that SID on Orbitrap platforms optimized for increased m/z range will also be beneficial to mass spectrometry users.

Herein, we present a combination of surface-induced dissociation and high-resolution mass analysis as applied to the study of protein complexes. An Exactive Plus Extended Mass Range (EMR) Orbitrap instrument (Thermo Fisher

Scientific, Bremen, Germany), modified with a high-mass quadrupole filter, was fitted with an SID device inspired by previous designs described in works by Wysocki et al.^{35,36} As with previous designs, the new device enables the instrument to perform SID experiments without interrupting the capability or performance of MS-only and CID experiments. The SID-Orbitrap platform was tested using several protein complexes with known quaternary structure. The resolving power of the Exactive Plus EMR platform was displayed through scrutiny of fragmentation products, revealing disparate oligomeric states of subunits that overlap one another in nominal m/z space and bound ligands retained through the SID process. Clear assignment of this nature was not possible in previous TOF studies without the assistance of IM.³⁰ Additional work investigating the localization of ligand binding by SID using the instrument described here was recently published and highlights additional applications and capabilities of the SID-Orbitrap instrument.³¹ The work presented here expands upon the utility of FT-based mass analysis in the field of native MS.

■ EXPERIMENTAL SECTION

SID Device Design. An SID device 4 cm in length was designed to replace the short multipole between the selection quadrupole and the C-trap in the modified EMR platform (Figure 1a–c). Importantly, this design will allow the device to also be used on the Q Exactive line of mass spectrometers, including the Q Exactive UHMR instrument. The electrode assembly was designed in Autodesk Inventor, and its performance was optimized using SIMION 8.1 software. Initial simulation parameters were chosen to reflect reasonable kinetic energy distributions and spatial distributions of precursor ions to better represent the ion beam within the mass spectrometer. Precursor and product ions were simulated using charge and mass values previously observed from SID experiments on various instrument platforms. An initial kinetic energy of 30–100 eV for precursor ions entering the SID device was used to simulate surface collisions over a range of lab frame energies. Because dissociation of precursor ions may occur after collision with the surface and before or after exiting the SID device, transmission of both precursor and product ions was considered following surface collisions. Upon collision with the surface, ions representative of product and precursor mass and charge values were formed, with kinetic energies ranging between 5 and 20% of the initial precursor kinetic energy. Collisions with background gas were not considered.

Fabrication of the device was carried out in-house by the OSU Department of Chemistry and Biochemistry machine shop, using aluminum for all electrodes and polyether ether ketone (PEEK) polymer to mount and properly space the electrodes. The original ion path remains unobstructed to allow for minimal impact on MS-only (i.e., no activation) experiments as well as CID (HCD) experiments. When SID is desired, the front-end electrodes of the SID device are tuned to direct ions to the surface at the top of the device. A detailed description of the surface used for collisions can be found elsewhere.³⁵ Briefly, a glass surface was coated with a 10 Å titanium layer and a 1000 Å gold layer and subsequently modified with a fluorocarbon self-assembled monolayer. Detailed drawings and voltages applied to the SID device can be found in Figure S1.

Mass Spectrometry. All experiments were carried out on an Exactive Plus EMR instrument that had been previously modified with a high-mass quadrupole filter that replaced the

original transfer multipole, similar to the modifications presented by Dyachenko et al.⁴⁰ All samples were ionized via static nanoelectrospray ionization using in-house pulled borosilicate capillaries and supplied with voltage via direct contact with a platinum wire. MS-only and CID experiments remained widely unaffected by the presence of the SID device in the instrument. In transmission mode, voltages are applied to the entrance and exit lens stacks on the SID device to assist with ion beam focusing between the quadrupole and the C-trap. A small loss of transmission is observed due to the lack of the rf-confining multipole; however, it should be noted that the SID device remains installed on our instrument without negatively affecting MS-only or CID experiments. Voltages applied to ion transfer optics throughout the mass spectrometer and the HCD cell pressure were adjusted to obtain optimal ion transmission while minimizing unintentional ion activation. Unless otherwise noted, CID was performed in the HCD cell, and all spectra were collected at 17 500 resolution as defined at 200 m/z . Quantitation of ligand-bound species and average charge state calculations were conducted using Protein Metrics Intact Mass deconvolution software⁴¹ and peak area integration, respectively.

SID is accomplished by applying repulsive and attractive DC voltages to the front bottom and front top lenses, respectively, to guide the ion beam to the surface for collisions. Subsequently, the ion beam is extracted off the surface and guided into the C-trap region by the rear lenses within the SID device. Voltages applied to the SID device are provided from a 10 channel DC power supply (Ardara Technologies, Ardara, PA). Detailed SID device tune settings for MS and MS/MS experiments can be found in Table S1. The fragment ions produced by SID can be trapped in the C-trap or allowed into the HCD cell for collisional cooling before returning to the C-trap region to be injected into the Orbitrap mass analyzer. The SID acceleration voltage is defined as the difference between the first SID entrance lens and the surface. The SID voltage range is afforded by applying a negative voltage to the C-trap DC offset during ion injection and accordingly increasing the available ΔV between SID entrance lenses and the surface (Figure S2ab). To achieve higher-energy SID capabilities, a modification to the ion optics board on the EMR instrument was required. Specifically, the voltage for the C-trap DC offset during ion injection steps had to be supplied by an external power supply to allow a larger range of voltages that can be applied to the C-trap offset during ion injection and therefore increase the acceleration voltage range of SID up to approximately 235 V. To increase the ease of use of the instrument, we designed a circuit that allows the user to switch between the on-board power supply for MS and HCD experiments and the external power supply for SID experiments (Figure S2c). It should be added that these modifications are relatively unobtrusive to the instrument and can be easily removed to produce a standard configuration, although removal of the SID device is not necessary for typical MS and CID experiments.

Materials. Protein complexes that have been characterized previously by SID in Q-TOF platforms^{30,42} were chosen to demonstrate the SID capabilities of the Orbitrap instrument modified in this work. Streptavidin (SA) was purchased from Thermo Scientific Pierce (Rockford, IL, USA), and glutamate dehydrogenase (GDH) from bovine liver was purchased from Millipore Sigma (St. Louis, MO, USA). The protein samples were buffer-exchanged into 100 mM ammonium acetate using

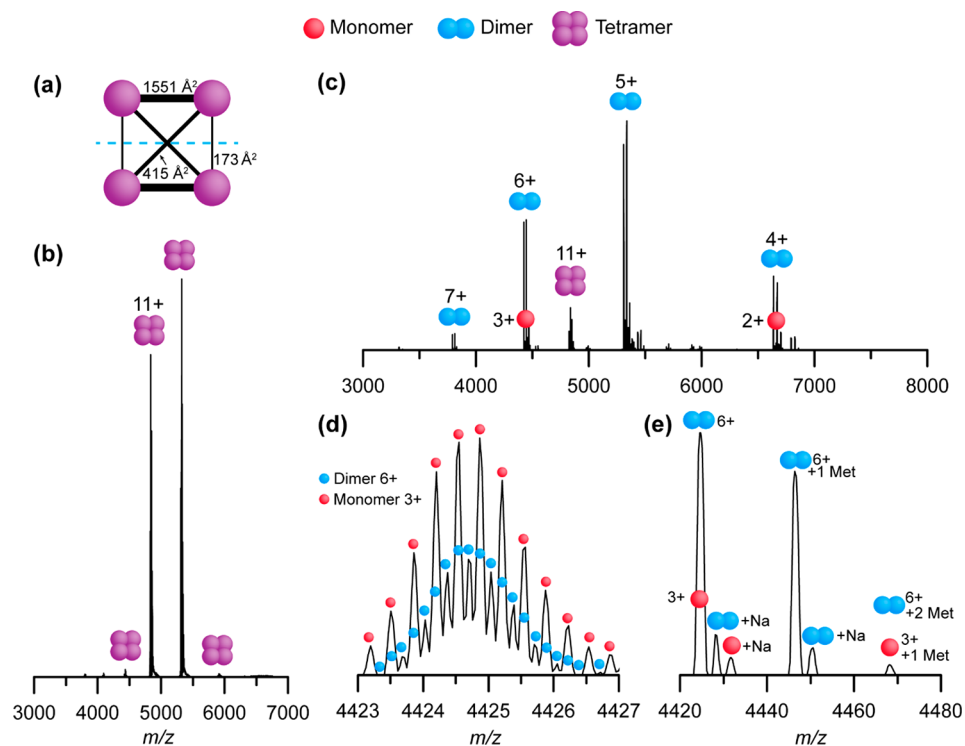


Figure 2. (a) Interface areas of streptavidin tetramer as determined by PISA analysis (PDB ID: 1SWB).⁴³ (b) Mass spectrum of streptavidin tetramer under charge-reducing conditions. (c) SID spectrum (45 V, 495 eV) of the 11+ tetramer. (d) A zoomed-in segment of (c) at 140 000 resolution setting, revealing the isotope distributions of the 3+ monomer and 6+ homodimer. (e) A zoomed-in segment of (c) at 17 500 resolution setting, showing noncleaved N-terminal methionine(s) and sodium adducts on the 3+ monomer and 6+ dimer.

Micro Bio-Spin P6 spin columns with a 6 kDa cutoff (Bio-Rad, Hercules, CA, USA) and subsequently adjusted with triethylammonium acetate (TEAA, Millipore Sigma) to a final buffer concentration of 80 mM ammonium acetate/20 mM TEAA. The addition of TEAA is used as a charge-reducing reagent, as it has been shown that reduced-charge precursor ions generally produce subcomplexes by SID that are more reflective of the complexes' native structure.⁴⁴ Protein concentrations were measured by A280 using a Nanodrop 2000C spectrophotometer (Thermo Fisher Scientific, Wilmington, DE, USA). The samples were diluted to a protein complex concentration of 2 μ M (SA tetramer) and 5 μ M (GDH hexamer) for mass spectrometry experiments. Streptavidin–biotin binding experiments were performed under identical conditions, with biotin (Millipore Sigma) added to make a 1.5:1 biotin to streptavidin monomer molar ratio.

RESULTS AND DISCUSSION

Streptavidin. Streptavidin serves as a model system for SID experiments. It is a 53 kDa D2 symmetric homotetramer, consisting of subunits arranged as a dimer of dimers (Figure 2a). Upon activation by CID, streptavidin tetramer dissociates into highly charged monomers and relatively low charged trimers (Figure S3).⁴⁵ This behavior where one subunit unfolds and takes with it a disproportionately large amount of charge is typical of CID because of its multistep energy deposition process.^{16–18} Importantly, this dissociation result from CID does not support the known dimer of dimers subunit arrangement. In contrast, previous work has shown that SID of a streptavidin tetramer results in the production of dimers at low energy and monomers at high energy, consistent

with the interface areas and complex geometry determined by crystal structure.³⁰

Charge states 11+ through 9+ are dominant for the streptavidin tetramer that is ionized from ammonium acetate/TEAA solution. The 11+ charge state was selected using the quadrupole mass filter and fragmented by SID (45 V, 495 eV), forming primarily dimers of charge state 5+ and 6+ (Figure 2b,c). Some ambiguity of product assignment in past SID experiments with TOF platforms has been resolved with the use of ion mobility to separate oligomeric states that overlap in m/z space (e.g., 3+ monomer and 6+ homodimer). In this instance, the high-resolution capabilities of the Orbitrap analyzer allowed for the direct observation of two SID products that overlap in nominal m/z space. Figure 2d shows the same 45 V (495 eV) SID spectrum recorded at high-resolution (140 000 resolution setting, 512 ms transient) displaying two isotope distributions over the same nominal m/z range, indicating the presence of 3+ monomers and 6+ homodimers. It should be noted that for higher-resolution measurements, the intensities of higher-order oligomers are artificially decreased relative to monomers because of a loss of coherence of the ion packet within the Orbitrap analyzer from increased collisions with background gas for species with larger cross sections and higher charge.⁴⁶ In fact, this phenomenon is so apparent that Sanders et al. have leveraged the transient decay rate of protein ions in the Orbitrap to make collision cross section measurements.⁴⁷ For this reason, we use low resolution (8750–35 000 as defined at 200 m/z) for acquisition of protein complexes and only use higher resolution for specific questions (i.e., small ligand binding, PTMs, etc.), being careful not to draw conclusions from the intensities of species at high resolution.

The bias favoring lower oligomeric states at high resolution is easily observed by comparing isotope distributions at high resolution in Figure 2d to a zoomed-in perspective of the 3+ monomer and 6+ dimer from a lower-resolution measurement in Figure 2e. While isotope distributions are no longer available at lower resolution, the presence of multiple oligomeric states can still be detected by examining the abundance of unremoved N-terminal methionine (Met) and sodium adducts on each signal. Streptavidin subunits can have incomplete Met removal on the N-terminus during protein expression, resulting in an observable distribution of peaks spaced by 131 Da.⁴⁸ A given oligomeric state of streptavidin will retain zero to n noncleaved Met residues (with n indicating the oligomeric state). Although the +3 monomer and +6 dimer overlap in m/z space, a dimer with one N-terminal methionine can easily be differentiated from a monomer with one N-terminal methionine. Furthermore, the presence of sodium adducts on each species can also be used to estimate the amount of dimer and monomer present in the SID spectrum (Figure 2e). Using this approach to assign oligomeric states of SID products, we observed that the ratio of streptavidin dimer to monomer is greater at lower resolution than at higher resolution. This bias as a function of transient time is even more obvious when comparing the SID products of 11+ streptavidin over a range of SID energies at both low and high resolution (Figure S4).

Ion Source Temperature Effects. Great emphasis in native MS lies in the retention of the physiological structure/structural features of proteins and protein complexes during analysis by using gentle instrument conditions for ionization, ion transfer, and detection. Unfortunately, as a result of such gentle instrument conditions, native ions have an increased tendency to carry adducts from nonvolatile salts and buffers. Excessive adducting often reduces the “apparent resolution” of the instrument far below what is attainable under denaturing conditions.⁴⁹ The source region on the Exactive line of instruments is often held at relatively high temperature (200–250 °C) to improve sensitivity and declustering of the ions as they enter the mass spectrometer. Although this drastically improves the apparent resolution and sensitivity of the instrument, it is often a concern that high source temperatures may result in restructuring of ions,⁵⁰ similar to what has been observed at low collision-induced dissociation energies.⁵¹ Here we use SID in an attempt to determine if high ion source temperatures affect the structure of protein complex ions.

In previous studies, SID has been shown to differentiate between native-like ions and ions that have undergone gross structural changes (i.e., collapse, expansion) via preactivation of the precursor ions, prior to dissociation.⁵² Notable differences in SID fragmentation were observed when precursor ions were activated prior to SID when compared to fragmentation without preactivation. This same sensitivity to preactivation is observed with the new SID device within the Q Exactive EMR platform, as expected—SID measures the system as it is presented, providing dissociation patterns that vary with extent of preactivation.

We chose to use the interaction of streptavidin tetramer with biotin to determine if ion source temperature affects the structure of the streptavidin tetramer. The streptavidin–biotin interaction is primarily mediated through hydrogen bonding and van der Waals interactions, although interactions with aromatic interactions also play a role.⁵³ Previous studies have suggested that the solution-specific interactions between streptavidin and biotin are largely preserved upon introduction

into the gas phase.⁵⁴ When streptavidin tetramer bound with four biotin ligands was analyzed over a range of ion source temperatures, it was observed that tetramer with four bound biotin was the dominant species even at source temperatures up to 300 °C (Figure 3a, S5). In dissociation experiments, 11+

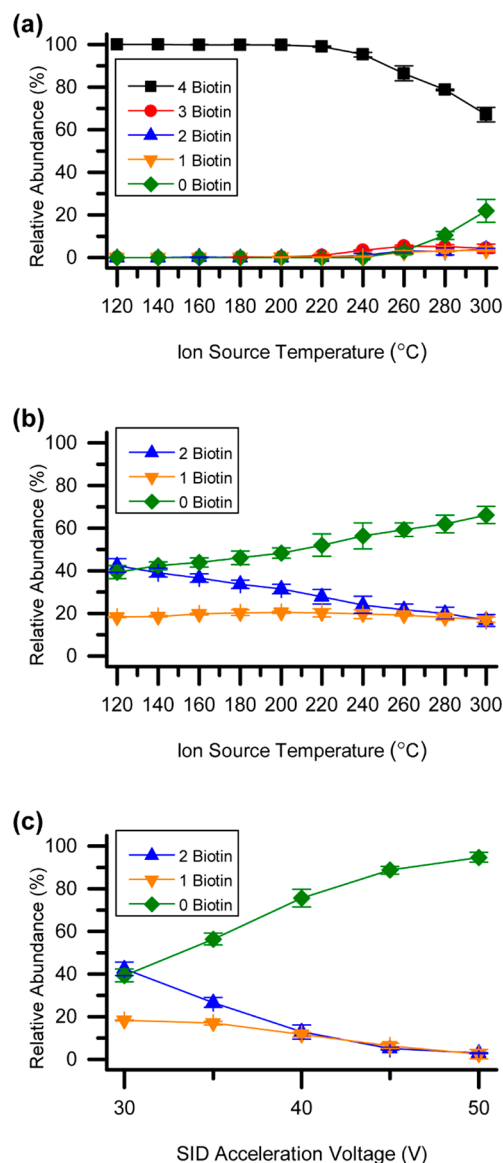


Figure 3. Plots comparing the relative degree of biotin retention on (a) streptavidin tetramers as a function of ion source temperature, (b) dimers produced by SID (30 V, 330 eV) of the streptavidin tetramers shown in part (a) as a function of ion source temperature, and (c) dimers produced from SID of the streptavidin–biotin tetramer as a function of SID acceleration voltage at a constant ion source temperature of 120 °C. In all cases, error bars are representative of the standard deviation of triplicate measurements.

streptavidin tetramer was selected and subjected to 30 V (330 eV) of SID. As with previous reports, dimer products were observed both with and without biotin retained (Figure S6).^{30,39} The Orbitrap EMR platform provides baseline resolution of the apo and holo species in m/z space, allowing for easy relative quantitation of ligand retention. The same SID experiment was performed with ion source temperatures ranging from 120 to 300 °C, resulting in a greater loss of

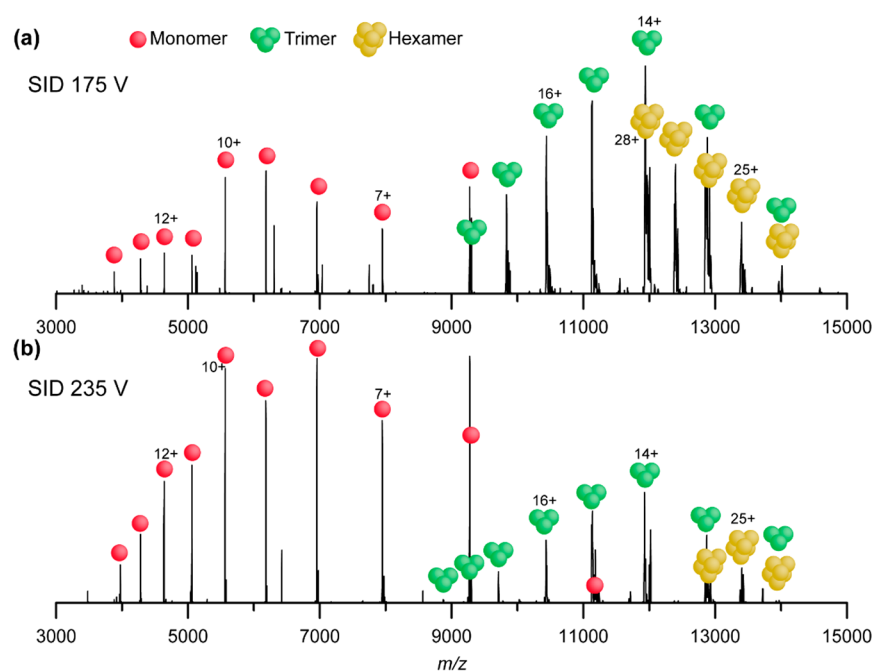


Figure 4. SID spectrum of +28 GDH hexamer at (a) 175 V and (b) 235 V SID acceleration voltage, resulting in trimers and monomers that are indicative of the overall dimer of trimers arrangement of GDH hexamer.

biotin from SID products as the ion source temperature was increased (Figure 3b, Figure S6). In contrast, even at the lowest ion source temperatures, when the 11+ streptavidin–biotin tetramer ion is subjected to CID, the biotin is completely lost before subunit dissociation occurs and exclusively apo-monomer and apo-trimer are observed at higher CID energies (Figure S7). Interestingly, the symmetry of charge partitioning of SID products does not significantly change as a function of ion source temperature, in contrast to an increase in asymmetric charge partitioning that might have been expected if significant structural changes had occurred (Figure S8). To determine if the loss of the biotin ligand could be an effect of precursor ion energy rather than a gross structural change, we collected SID spectra of 11+ streptavidin–biotin tetramer at additional SID energies with an ion source temperature of 120 °C (Figures 3c, and S9). These results made it obvious that biotin retention is drastically affected by the energy of the ion–surface collision process, with almost complete biotin loss observed at SID energies of 550 eV (50 V). As no significant increase in asymmetric charge partitioning of the SID produced dimers is observed at high ion source temperatures, it is possible that the loss of biotin at high source temperatures is a result of increased vibrational energy of the precursor ion prior to SID and not necessarily a significant structural change during preactivation. This finding is consistent with gross structure retention at elevated source temperature as presented in a recent publication that describes the use of the SID-Orbitrap EMR instrument to monitor ligand retention in protein complexes.³¹ Although we do not observe evidence of any gross structural changes during the preactivation step, further investigations will need to be completed to fully understand the complex-dependent effect of ion source temperature on the structure of native protein complexes in the Exactive line of mass spectrometers. Further technological advances such as the implementation of ion mobility on the Exactive mass spectrometers may be critical in this understanding.⁵⁵

L-Glutamate Dehydrogenase. Bovine glutamate dehydrogenase (GDH) is a 333.6 kDa homohexameric enzyme arranged as a stacked dimer of trimers with a coiled antenna protruding from and stabilizing each trimer.^{56,57} Previous studies have shown that GDH is difficult to dissociate in the gas phase by CID, often requiring high CID energies and high precursor charge states, resulting in the ejection of an unfolded monomer that is not representative of the initial subunit arrangement.^{42,58} In contrast, it has previously been shown that SID of GDH hexamer on a Q-IM-TOF platform primarily resulted in the dissociation of GDH hexamer into trimers with secondary dissociation into monomers.⁴² Furthermore, Ma et al. showed that under charge-reducing conditions (addition of TEAA), the trimers and monomers produced from SID of GDH hexamer remain compact and have collision cross sections similar to those expected for native-like GDH subcomplexes clipped from the crystal structure of hexamer. These results show that unlike CID, SID can be used to elucidate the topology of GDH hexamer.

Nano-electrospray of GDH hexamer in ammonium acetate/TEAA solution results in a charge state distribution with the 27+ charge state as the dominant peak (Figure S10a). Under these charge-reducing conditions, the maximum CID acceleration voltage of 200 V on the EMR platform does not result in dissociation of the 28+ hexamer but instead only leads to minor charge stripping (Figure S10b). In contrast, subjecting the 28+ GDH hexamer to 175 V (4900 eV) SID yields abundant trimer and a bimodal charge state distribution of monomer subcomplexes as well as charge stripped hexamer (Figure 4a). The presence of symmetrically charged trimers supports the hypothesis by Ma et al. that GDH fragments by SID to form trimers without significant structural rearrangement.⁴² Higher-energy SID (235 V, 6580 eV) results in an increase in the low-charged monomer distribution, (Figure 4b). It is unsurprising that the monomer ions do not exhibit the symmetric charge partitioning typical of SID products, as the intertwined sections of each monomer need to unravel

prior to dissociation. We hypothesize that the higher-charged monomers likely originate from direct dissociation of hexamer to monomer and pentamer, where the complementary pentamers are not detected due to decreased transmission at high m/z in the EMR instrument. It is possible that the lower-charged monomers are a result of secondary dissociation from trimers or that they are a product of a different gas-phase conformation of the hexamer ions. These results suggest that the major products of SID reflect the topology of GDH hexamer, as the interactions between the trimer–trimer interface are broken at moderate energies, and the interactions between individual subunits within the trimer that are strengthened by the coiled helical tails present within each trimer are broken at higher energies. The discrimination of high m/z products on the EMR instrument is expected to be less of a problem on the recently released Q Exactive UHMR instrument, and this will be tested and reported once we have optimized SID in that instrument. In addition, the high-resolution capabilities of the Orbitrap instrument allow easy assignment of GDH subcomplexes without the use of additional methods such as ion mobility.

CONCLUSIONS

SID has been implemented in place of the transfer multipole in an Exactive Plus EMR Orbitrap instrument that has also been modified with a quadrupole mass filter. The SID device can be operated in place of the transfer multipole for ion transmission or can be used for surface collisions. Importantly, the SID device does not significantly affect ion transmission during CID or MS-only experiments, allowing the device to remain installed in the instrument for non-SID experiments. Well-studied multimeric protein and protein–ligand model complexes with different overall structures were successfully fragmented by SID and compare favorably with results previously acquired on time-of-flight platforms. The high mass resolving power inherent to the Orbitrap platform makes it possible to resolve oligomeric states with different mass and charge states that overlap in nominal m/z space by directly resolving the isotope envelope of each species. Furthermore, the extent of ligand binding to protein that was previously difficult to determine in SID experiments performed on TOF platforms is now clearly identifiable. The SID-Orbitrap platform has the potential to probe the effects of small ligands or protein modifications on the overall structure and stability of biomacromolecular complexes and is a powerful combination for the study of biomolecules of unknown structures.

ASSOCIATED CONTENT

Supporting Information

The Supporting Information is available free of charge on the ACS Publications website at DOI: 10.1021/acs.analchem.8b05605.

Detailed SID device drawings and voltages. Diagram of switching circuit for external power supply. MS-only and CID spectra of streptavidin and GDH. Spectra of streptavidin acquired over a range of SID energies. Spectra of biotin bound to streptavidin tetramer before SID and dimers after SID. Comparison of biotin binding to streptavidin dimer as a function of ion source temperature and SID energy. CID of streptavidin–biotin tetramer. Average charge state values for streptavidin–biotin dimers (PDF)

AUTHOR INFORMATION

Corresponding Author

*E-mail: wysocki.11@osu.edu; Phone: 1-614-292-8687.

ORCID

Zachary L. VanAernum: 0000-0002-0956-3956

Present Address

^{||}Thermo Fisher Scientific Inc., 5350 NE Dawson Creek Dr., Hillsboro, Oregon 97124, United States (J.D.G.)

Author Contributions

[§]Z.L.V. and J.D.G. contributed equally to this work.

Notes

The authors declare the following competing financial interest(s): J.D.G., M.E.B., A.A.M., and S.R.H. are employees of Thermo Fisher Scientific Inc.

ACKNOWLEDGMENTS

The authors thank Mr. Larry Antal (OSU Department of Chemistry and Biochemistry Machine Shop) and Mr. Eric Jackson (OSU Department of Chemistry and Biochemistry Instrument Support Group) for assistance with SID device manufacture and switching circuit design; Maria Reinhardt-Szyba, Dmitry Boll, Alexander Kholomeev, Jan-Peter Hauschild, and Eugen Damoc (Thermo Fisher Scientific) for assistance and helpful discussions regarding instrument modifications; Randy Pedder (Ardara Technologies) for helpful electronics discussions and support; Royston Quintyn and Lindsay Morrison for initial SID experiments on the Orbitrap platform using a different design; Marshall Bern (Protein Metrics Inc.) for assistance with spectral deconvolution and relative quantitation; and Jacob McCabe (Texas A&M University) and Benjamin Jones (The Ohio State University) for assistance with batch processing of average charge state calculations. The authors gratefully acknowledge financial support from the National Science Foundation (NSF 1455654 to V.H.W.) and from the National Institutes of Health (NIH P41GM128577 to V.H.W.).

REFERENCES

- (1) Spirin, V.; Mirny, L. A. *Proc. Natl. Acad. Sci. U. S. A.* **2003**, *100* (21), 12123–12128.
- (2) Heck, A. J. R. *Nat. Methods* **2008**, *5* (11), 927–933.
- (3) Liko, I.; Allison, T. M.; Hopper, J. T.; Robinson, C. V. *Curr. Opin. Struct. Biol.* **2016**, *40*, 136–144.
- (4) Lössl, P.; van de Waterbeemd, M.; Heck, A. J. *EMBO J.* **2016**, *35*, 2634.
- (5) Sobott, F.; Hernández, H.; McCammon, M. G.; Tito, M. A.; Robinson, C. V. *Anal. Chem.* **2002**, *74* (6), 1402–1407.
- (6) van denHeuvel, R. H. H.; van Duijn, E.; Mazon, H.; Synowsky, S. A.; Lorenzen, K.; Versluis, C.; Brouns, S. J. J.; Langridge, D.; van der Oost, J.; Hoyes, J.; et al. *Anal. Chem.* **2006**, *78* (21), 7473–7483.
- (7) Li, H.; Wolff, J. J.; Van Orden, S. L.; Loo, J. A. *Anal. Chem.* **2014**, *86* (1), 317–320.
- (8) Rose, R. J.; Damoc, E.; Denisov, E.; Makarov, A.; Heck, A. J. R. *Nat. Methods* **2012**, *9* (11), 1084–1086.
- (9) Fort, K. L.; van de Waterbeemd, M.; Boll, D.; Reinhardt-Szyba, M.; Belov, M. E.; Sasaki, E.; Zschoche, R.; Hilvert, D.; Makarov, A. A.; Heck, A. J. R. *Analyst* **2018**, *143*, 100.
- (10) Snijder, J.; van de Waterbeemd, M.; Damoc, E.; Denisov, E.; Grinfeld, D.; Bennett, A.; Agbandje-McKenna, M.; Makarov, A.; Heck, A. J. R. *J. Am. Chem. Soc.* **2014**, *136* (20), 7295–7299.
- (11) van de Waterbeemd, M.; Fort, K. L.; Boll, D.; Reinhardt-Szyba, M.; Routh, A.; Makarov, A.; Heck, A. J. R. *Nat. Methods* **2017**, *14* (3), 283–286.
- (12) Sharon, M. *J. Am. Soc. Mass Spectrom.* **2010**, *21* (4), 487–500.

- (13) Skinner, O. S.; Haverland, N. A.; Fornelli, L.; Melani, R. D.; Do Vale, L. H. F.; Seckler, H. S.; Doubleday, P. F.; Schachner, L. F.; Szrentić, K.; Kelleher, N. L. *Nat. Chem. Biol.* **2017**, *14*, 36.
- (14) Skinner, O. S.; Havugimana, P. C.; Haverland, N. A.; Fornelli, L.; Early, B. P.; Greer, J. B.; Fellers, R. T.; Durbin, K. R.; Do Vale, L. H. F.; Melani, R. D.; et al. *Nat. Methods* **2016**, *13* (3), 237–240.
- (15) Benesch, J. L. P.; Ruotolo, B. T.; Simmons, D. A.; Robinson, C. V. *Chem. Rev.* **2007**, *107* (8), 3544–3567.
- (16) Felitsyn, N.; Kitova, E. N.; Klassen, J. S. *Anal. Chem.* **2001**, *73* (19), 4647–4661.
- (17) Jurchen, J. C.; Williams, E. R. *J. Am. Chem. Soc.* **2003**, *125* (9), 2817–2826.
- (18) Popa, V.; Trecroce, D. A.; McAllister, R. G.; Konermann, L. J. *Phys. Chem. B* **2016**, *120* (23), 5114–5124.
- (19) Dixit, S. M.; Polasky, D. A.; Ruotolo, B. T. *Curr. Opin. Chem. Biol.* **2018**, *42*, 93–100.
- (20) Lermite, F.; Sobott, F. *Proteomics* **2015**, *15* (16), 2813–2822.
- (21) Zhang, H.; Cui, W.; Wen, J.; Blankenship, R. E.; Gross, M. L. *Anal. Chem.* **2011**, *83* (14), 5598–5606.
- (22) Skinner, O. S.; McAnally, M. O.; Van Duyne, R. P.; Schatz, G. C.; Breuker, K.; Compton, P. D.; Kelleher, N. L. *Anal. Chem.* **2017**, *89* (20), 10711–10716.
- (23) Geels, R. B. J.; van der Vies, S. M.; Heck, A. J. R.; Heeren, R. M. A. *Anal. Chem.* **2006**, *78* (20), 7191–7196.
- (24) O'Brien, J. P.; Li, W.; Zhang, Y.; Brodbelt, J. S. *J. Am. Chem. Soc.* **2014**, *136* (37), 12920–12928.
- (25) Morrison, L. J.; Brodbelt, J. S. *J. Am. Chem. Soc.* **2016**, *138*, 10849.
- (26) Tamara, S.; Dyachenko, A.; Fort, K. L.; Makarov, A. A.; Scheltema, R. A.; Heck, A. J. R. *J. Am. Chem. Soc.* **2016**, *138*, 10860.
- (27) Zhou, M.; Wysocki, V. H. *Acc. Chem. Res.* **2014**, *47* (4), 1010–1018.
- (28) Beardsley, R. L.; Jones, C. M.; Galhena, A. S.; Wysocki, V. H. *Anal. Chem.* **2009**, *81* (4), 1347–1356.
- (29) Zhou, M.; Dagan, S.; Wysocki, V. H. *Angew. Chem., Int. Ed.* **2012**, *51* (18), 4336–4339.
- (30) Quintyn, R. S.; Yan, J.; Wysocki, V. H. *Chem. Biol.* **2015**, *22* (5), 583–592.
- (31) Busch, F.; VanAernum, Z. L.; Ju, Y.; Yan, J.; Gilbert, J. D.; Quintyn, R. S.; Bern, M.; Wysocki, V. H. *Anal. Chem.* **2018**, *90* (21), 12796–12801.
- (32) Song, Y.; Nelp, M. T.; Bandarian, V.; Wysocki, V. H. *ACS Cent. Sci.* **2015**, *1* (9), 477–487.
- (33) Romano, C. A.; Zhou, M.; Song, Y.; Wysocki, V. H.; Dohnalkova, A. C.; Kovarik, L.; Paša-Tolić, L.; Tebo, B. M. *Nat. Commun.* **2017**, *8* (1), 746.
- (34) Zhou, M.; Yan, J.; Romano, C. A.; Tebo, B. M.; Wysocki, V. H.; Paša-Tolić, L. *J. Am. Soc. Mass Spectrom.* **2018**, *29*, 723.
- (35) Galhena, A. S.; Dagan, S.; Jones, C. M.; Beardsley, R. L.; Wysocki, V. H. *Anal. Chem.* **2008**, *80* (5), 1425–1436.
- (36) Zhou, M.; Huang, C.; Wysocki, V. H. *Anal. Chem.* **2012**, *84* (14), 6016–6023.
- (37) Gault, J.; Donlan, J. A. C.; Liko, I.; Hopper, J. T. S.; Gupta, K.; Housden, N. G.; Struwe, W. B.; Marty, M. T.; Mize, T.; Bechara, C.; et al. *Nat. Methods* **2016**, *13* (4), 333–336.
- (38) Liko, I.; Degiacomi, M. T.; Lee, S.; Newport, T. D.; Gault, J.; Reading, E.; Hopper, J. T. S.; Housden, N. G.; White, P.; Colledge, M.; et al. *Proc. Natl. Acad. Sci. U. S. A.* **2018**, *115*, 6691–6696.
- (39) Yan, J.; Zhou, M.; Gilbert, J. D.; Wolff, J. J.; Somogyi, Á.; Pedder, R. E.; Quintyn, R. S.; Morrison, L. J.; Easterling, M. L.; Paša-Tolić, L.; et al. *Anal. Chem.* **2017**, *89* (1), 895–901.
- (40) Dyachenko, A.; Wang, G.; Belov, M.; Makarov, A.; de Jong, R. N.; van den Bremer, E. T. J.; Parren, P. W. H. I.; Heck, A. J. R. *Anal. Chem.* **2015**, *87* (12), 6095–6102.
- (41) Bern, M.; Caval, T.; Kil, Y. J.; Tang, W.; Becker, C.; Carlson, E.; Kletter, D.; Sen, K. I.; Galy, N.; Hagemans, D.; et al. *J. Proteome Res.* **2018**, *17* (3), 1216–1226.
- (42) Ma, X.; Zhou, M.; Wysocki, V. H. *J. Am. Soc. Mass Spectrom.* **2014**, *25* (3), 368–379.
- (43) Krissinel, E.; Henrick, K. *J. Mol. Biol.* **2007**, *372* (3), 774–797.
- (44) Zhou, M.; Dagan, S.; Wysocki, V. H. *Analyst* **2013**, *138* (5), 1353.
- (45) Schwartz, B. L.; Bruce, J. E.; Anderson, G. A.; Hofstadler, S. A.; Rockwood, A. L.; Smith, R. D.; Chilkoti, A.; Stayton, P. S. *J. Am. Soc. Mass Spectrom.* **1995**, *6* (6), 459–465.
- (46) Makarov, A.; Denisov, E. *J. Am. Soc. Mass Spectrom.* **2009**, *20* (8), 1486–1495.
- (47) Sanders, J. D.; Grinfeld, D.; Aizikov, K.; Makarov, A.; Holden, D. D.; Brodbelt, J. S. *Anal. Chem.* **2018**, *90* (9), 5896–5902.
- (48) Wingfield, P. T. *Curr. Protoc. Protein Sci.* **2017**, *88* (1), 6.14.1–6.14.3.
- (49) Lössl, P.; Snijder, J.; Heck, A. J. R. *J. Am. Soc. Mass Spectrom.* **2014**, *25* (6), 906–917.
- (50) Pacholarz, K. J.; Barran, P. E. *Anal. Chem.* **2015**, *87* (12), 6271–6279.
- (51) Benesch, J. L. P. *J. Am. Soc. Mass Spectrom.* **2009**, *20* (3), 341–348.
- (52) Quintyn, R. S.; Zhou, M.; Yan, J.; Wysocki, V. H. *Anal. Chem.* **2015**, *87* (23), 11879–11886.
- (53) Stenkamp, R. E.; Trong, I. L.; Klumb, L.; Stayton, P. S.; Freitag, S. *Protein Sci.* **1997**, *6* (6), 1157–1166.
- (54) Deng, L.; Broom, A.; Kitova, E. N.; Richards, M. R.; Zheng, R. B.; Shoemaker, G. K.; Meiering, E. M.; Klassen, J. S. *J. Am. Chem. Soc.* **2012**, *134* (40), 16586–16596.
- (55) Poltash, M. L.; McCabe, J. W.; Shirzadeh, M.; Laganowsky, A.; Clowers, B. H.; Russell, D. H. *Anal. Chem.* **2018**, *90*, 10472.
- (56) Peterson, P. E.; Smith, T. J. *Structure* **1999**, *7* (7), 769–782.
- (57) Smith, T. J.; Peterson, P. E.; Schmidt, T.; Fang, J.; Stanley, C. A. *J. Mol. Biol.* **2001**, *307* (2), 707–720.
- (58) Han, L.; Ruotolo, B. T. *Anal. Chem.* **2015**, *87* (13), 6808–6813.